



Two typical merging events of oceanic mesoscale anticyclonic eddies

Zi-Fei Wang¹, Liang Sun¹, Qiu-Yang Li¹, Hao Cheng¹

¹ School of Earth and Space Sciences, University of Science and Technology of China, Hefei, Anhui, 230026, PR China

Correspondence to: Liang Sun (sunl@ustc.edu.cn)

5 **Abstract.** The long-term theoretical “energy paradox” of whether the final state of two merging anticyclones contains more energy than the initial state is studied by observing two typical merging events of ocean mesoscale eddies. It is found that the total mass (volume), total circulation (area integration of vorticity) and total angular momentum (AM) are conserved if the orbital AM relative to the center of mass is taken into account as the eddies rotate around the center of mass before merging. For subsurface merging, the mass trapped by the Taylor–Proudman effect above the subsurface eddies should also be included. 10 Both circulation conservation laws and orbital AM have been overlooked in previous theoretical studies. The total eddy kinetic energy slightly decreases after merging due to fusion. On the contrary, the total eddy potential energy (EPE) significantly increases after the merging. The increase of the EPE is mostly supported by the loss of gravitational potential energy (PE) via eddy sinking below the original level. This implies that the merging of eddies requires the background gravitational PE to convert to the EPE. In contrast, the vorticity and enstrophy consequently decrease after merging. Thus, the eddy merging effect 15 behaves as a “large-scale energy pump” in an inverse energy cascade. It is noted that eddy conservation and conversion laws depend on laws of physical dynamics, even if additional degrees of freedom can be provided in a mathematical model.

1 Introduction

Mesoscale eddies usually have a long life cycle of weeks or months, and carry long-distance transports of heat, salt, and other passive tracers [Chelton et al., 2011a; Dong et al., 2014; McGillicuddy et al., 2011; Zhang et al., 2014] by trapping them, since 20 they are ubiquitous and are the most energetic component in the ocean. During their lifetime, complex dynamic processes occur, such as merging and splitting, which are associated with an eddy’s genesis and termination. This in turn modulates the eddy’s life cycle and its transports.

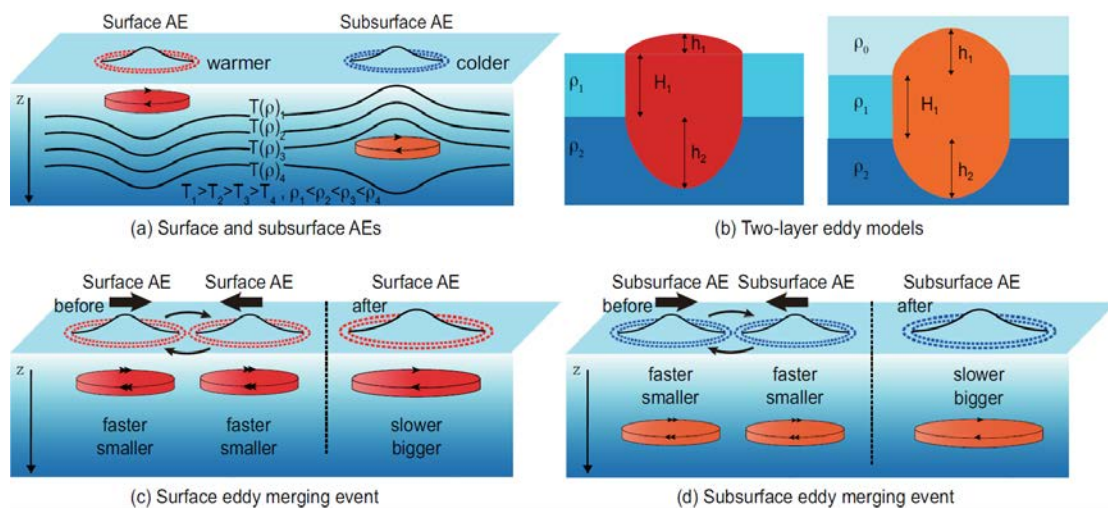
There is a long-term unresolved “paradox” regarding the merging of two like-signed oceanic mesoscale eddies, i.e., whether the merged eddy has more or less energy than before? This paradox first emerged from a theoretical study on the merging of 25 two anticyclonic, zero-potential-vorticity plane eddies by Gill and Griffiths [Nof and Simon, 1987; Cushman-Roisin 1989; Lumpkin et al., 2000]. According to the theory, if mass and potential vorticity are conserved by two anticyclones, the final state should contain more energy than the initial state, which implies that an additional source of energy must be supplied to complete the process. This study seemed to open a “Pandora’s box,” as the following studies are contradiction in which eddy properties (mass, potential vorticity, energy, angular momentum) should be conserved after merging. The



30 conservation of mass is a generally accepted assumption and was validated in experiments [Nof and Simon, 1987].
 However, there are still some merging scenarios where mass is not conserved [Cushman-Roisin 1989; Lumpkin et al.,
 2000].

Similarly, the conservation of potential vorticity (PV) [Gill and Griffiths 1981; Cushman-Roisin 1989; Nof, 1990] is
 abandoned in other studies [Griffiths and Hopfinger 1987; Nof and Simon, 1987; Nof, 1988; Lumpkin et al., 2000]. In
 35 contrast, the previously overlooked conservation of angular momentum (AM) [Cushman-Roisin 1989] becomes generally
 accepted in various following models [Nof, 1990; Pavia and Cushman-Roisin 1990; Lumpkin et al., 2000]. Consequently, in
 theoretical merging scenarios, the merged eddy might have less [Lumpkin et al., 2000], equal [Nof and Simon, 1987; Pavia
 and Cushman-Roisin, 1990; Lumpkin et al., 2000], or more energy [Griffiths and Hopfinger 1987] than before, depending
 on the assumptions. Since these eddy models only have two parameters (amplitude and radius), there was a dilemma that
 40 parameters are less than conservation laws (e.g., mass, vorticity, momentum, energy) [Pavia and Cushman-Roisin, 1990;
 Lumpkin et al., 2000]. This leads again to the question of which conservation laws should be applied in eddy merging
 [Lumpkin et al., 2000]. One possible way to solve the dilemma is to use a complex eddy model with more parameters, with
 which more conservation laws might be simultaneously held.

In addition, an effective way to dispel this “paradox” in eddy merging scenarios is to use oceanic observations to examine the
 45 above assumptions. However, this was seldom studied previously, since the filed observations by voyage and floats can hardly
 capture the eddy merging events, except for only a few cases [Cresswell, 1982; Sangra et al., 2005]. On the other hand, satellite
 observations provide another way of observing eddy motions. Based on sea level anomaly (SLA) data, the Genealogical
 Evolution Model (GEM), an efficient logical model, was developed to track dynamic evolution (merging and splitting) of
 eddies [Li et al., 2014; Li et al., 2016].



50

Figure 1. (a) Surface and subsurface anticyclonic eddies, (b) two-layer eddy models used in the present study, (c) surface eddy merging event, and (d) subsurface eddy merging event.



The motivation of this study is to test the conservation laws without any assumption by calculating the eddy properties. To this
55 end, we firstly chose two typical merging events by using GEM. Next, eddies were distinguished as surface and subsurface
eddies (Fig. 1a) according to sea surface temperature (SST) data [Assassi et al. 2016]. Secondly, we used a vertical two-layer
model (Fig. 1b) [Lumpkin et al., 2000] and a Gaussian model for horizontal shape according to observations [Wang et al.,
2015, Yi et al., 2015]. The eddy parameters are much more than potential conservation laws, to avoid the above dilemma.
Thirdly, we estimated eddy parameters pre- and post-merging (Fig. 1c, d) with a nonlinear optimal fitting approach [Wang et
60 al., 2015]. Finally, we calculated the eddy properties to determine what occurs after eddy merging.

2. Data and Method

2.1 Data

The SLA data used here were from the merged and gridded satellite product of MSLA (Maps of SLA), which were produced
and distributed by AVISO (<http://www.avisooceanobs.com/>) based on TOPEX/Poseidon, Jason-1, ERS-1, and ERS-2 data
65 [Ducet et al., 2000]. Currently, the products are available on a daily scale with a $0.25^\circ \times 0.25^\circ$ resolution in the global ocean
as DUACS DT14 [Pujol et al., 2016].

The SST data is produced from the Operational Sea Surface Temperature and Sea Ice Analysis (OSTIA) system [Donlon et
al., 2011], and downloaded on Asia-Pacific Data-Research Center (APDRC <http://apdrc.soest.hawaii.edu/data/>). The analysis
of SST data has global coverage with a spatial resolution of $0.05^\circ \times 0.05^\circ$ and a temporal resolution of 1 day. The ocean
70 vertical density profile data is from NCEP Global Ocean Data Assimilation System (GODAS) [Behringer et al., 2004], and
downloaded from NOAA (<https://www.esrl.noaa.gov/psd/data/gridded/data.godas.html>).

Eddy merging events were tracked using the GEM model [Li and Sun, 2015; Li et al, 2016], which is an efficient logical
model for tracking the dynamic evolution of mesoscale eddies (merging and splitting) from satellite SLA data.

2.2 Identification of surface and subsurface anticyclonic eddies

75 Surface eddies are distinguished from subsurface eddies by whether their core is in the surface layer or located inside the water
column (Fig. 1a). Consequently, surface anticyclonic eddies (AEs) have positive SST anomalies (SSTAs) while subsurface
AEs have negative SSTA [Assassi et al, 2016]. Here, we use the method proposed by Assassi et al. (2016) to identify the
surface AE and subsurface AE by using the SSTA. If SSTA index > 0 (SSTA index < 0), then the eddy is identified as a surface
(subsurface) AE. The SSTA is obtained by removing the background SST, which is the weighted-average of the SST within
80 the $4.5^\circ \times 4.5^\circ$ box, as previously used.



2.3 Eddy parameters

In this study, we use a Gaussian model for SLAs to obtain the eddy properties, which is the most typical model for ocean mesoscale eddies [Wang et al., 2015]. The SLA field $h(x,y)$ with several adjacent eddies before merging can be expressed as [Yi et al, 2015]

$$85 \quad h(x,y) = b + \sum_{i=1}^n A_i \times \exp\left[\frac{(x-x_{0i})^2}{L_x^2} + \frac{(y-y_{0i})^2}{L_y^2}\right] \quad (1)$$

where x, y are the zonal and meridional coordinates, respectively; x_0, y_0 is the position of the eddy center; L_x and L_y correspond to the longitude and latitude radii, respectively; and A denotes the eddy amplitude. The eddy parameters (A, L_x , and L_y) are obtained by using nonlinear fitting [Wang et al., 2015]. The eddy size, i.e., eddy area $S = \pi L_x L_y$, is calculated by integrating an ellipse. It is useful to point out that eddy area but eddy radii is an extensive quantity; this is the reason why the eddy area is
 90 the intrinsic parameter in estimating eddy viscosity [Li et al., 2018]. Next, the velocity (u, v) and vorticity (ξ) of the eddy field is calculated with geostrophic approximation. The parameter b represents the vertical eddy shift, which is critical for properly compositing and fitting the eddy parameters [Wang et al., 2015]. In addition, we point out for the first time that it is associated with PE conversion balance in this study.

For a two-layer model, as shown in Fig. 1b, the upper (lower) layer has a thickness of H_1 (H_2) and a density of ρ_1 (ρ_2). The
 95 surface AE consists of three parts—the upper surface h_1 , the lower surface h_2 , and the eddy body of height H_1 . Typically, we have $h_1 \ll h_2 \ll H_1$. If both h_1 and h_2 are too small to be ignored, the model becomes a one-layer model of a cylinder [Sangra et al., 2005] or a plane model, as used in many previous theoretical models. On the other hand, if H_1 is too small to be ignored, it becomes a lens model [e.g., Lumpkin et al., 2000]. For subsurface AEs, there is an additional surface layer of thickness H_0 and density ρ_0 over the eddy (Fig. 1b). In the present study, both H_0 and H_1 are chosen to be 200 m, partly according to some
 100 recent observations [Zhang et al., 2015; Bashmachnikov 2017; Li et al., 2017].

2.4 Eddy properties

The eddy properties are calculated by integration of proper parameters. As the density varies little from surface to deep sea, the anticyclone mass is calculated by numerical integration of volume:

$$V = \iint (H_1 + h_1 + h_2) dx dy \quad (2)$$

105 where H_1 is the depth of vortex body layer, and h_1 and h_2 are the upper and lower interface anomalies, as shown in Fig. 1b. The relative eddy circulation Γ is calculated by integration of PV:

$$\Gamma = \iint \left(\frac{f+\xi}{H_1+h_1+h_2} - \frac{f}{H_1} \right) (H_1 + h_1 + h_2) dx dy \quad (3)$$

where f is the Coriolis parameter. The relative PV mean $\xi_m = \Gamma/S$ is the area average of circulation Γ . The relative AM is calculated by integration of torque:

$$110 \quad L = \iint (vx - uy)(H_1 + h_1 + h_2) dx dy \quad (4)$$

The eddy kinetic energy (EKE) per mass is calculated by integration as follows:



$$E_k = \iint \left(\frac{u^2 + v^2}{2} \right) (H_1 + h_1 + h_2) dx dy \quad (5)$$

The eddy potential energy (EPE) consists of the effective PE of the upper interface and the lower interface:

$$E_p = \iint \left(\frac{1}{2} g_1' h_1^2 + \frac{1}{2} g_2' h_2^2 \right) dx dy \quad (6)$$

115 where g_1' and g_2' are the reduced gravity. The eddy enstrophy is calculated by integration:

$$E_s = \iint \left(\frac{1}{2} \xi^2 \right) dx dy \quad (7)$$

3. Results

3.1 Merging of surface AEs

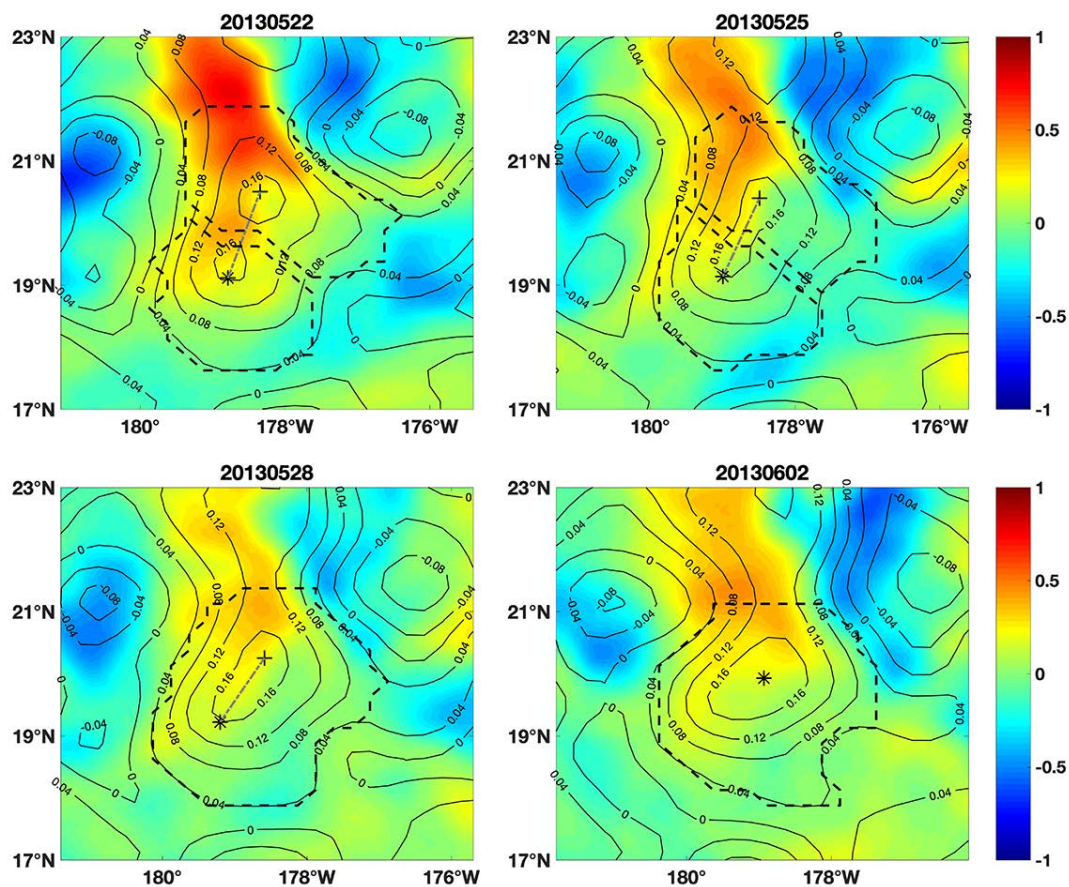
The first merging event consists of two AEs (AE1 and AE2) at the south of the Kuroshio Extension within from 17° to 22° N
120 and 180° to 174° W from May 19, 2013 to June 10, 2013 (Fig. 2). Before merging, AE1 was located at approximately 178° W
and 19° N, and AE2 was located to its north-east (Fig. 2a). Since both eddies have positive SSTAs, they are surface AEs, as
mentioned in section 2. Both eddies then moved westward from 178° W to 179° W (Fig. 2d). During this time, AE1 and AE2
co-rotated anticyclonically. This co-rotation was also observed by Li et al., (2016). Next, AE1 and AE2 eventually merged
into a larger eddy AE on June 1st (Fig. 2c). In this case, the upper (lower) layer, ranging from 0 to 200 m (200 to 1000 m)
125 depth, has a mean density of 1024.2 (1029.4) kg/m³, according to GODAS data for this region. The height of the eddy body
 H_1 is 200 m, and the lower surface height h_2 is approximately 195 times that of the eddy amplitude h_1 .

To clearly illustrate what occurred for eddies during the merging process, we first calculated both eddy parameters. It is obvious
that both eddies had positive SSTAs, and that the merged eddy AE also had positive SSTAs (Fig. 3a). They all were surface
AEs. The fitted eddy parameters are shown in Fig. 3a. The first fitted parameter is the vertical shift b , representing the
130 background SLA. In this case, b was very small, and decreased a small amount, from approximately 0.045 m before merging
to 0.038 m after merging. The second parameter is the amplitude of the eddy. Before merging, the amplitude of AE2 gradually
increased from 0.12 m to 0.14 m and, notably, the amplitude of AE1 gradually decreased from 0.12 m to 0.08 m. After merging,
the amplitude of the merged eddy also continually increased from 0.16 m to 0.17 m. In contrast, the area of both eddies seldom
changed before merging. AE2 had a large area of 1.7×10^4 km², while AE1 had a smaller area of 0.9×10^4 km².

135 Next, we calculated the eddy properties using the above parameters. The mass (volume) of eddies had changes similar to those
of the eddy area (Fig. 3b). This is because H_1 dominates the whole depth as $h_1 \ll h_2 \ll H_1$. The relative PV is averaged within
each eddy. As shown in Fig. 3b, the vorticity of AE2 varied by a very small amount, and the vorticity of AE1 gradually
decreased before merging. It is noted that the vorticity of AE2 is significantly smaller, although it had a larger amplitude. This
is because vorticity is not only proportional to amplitude, but is also inversely proportional to area. After merging, the vorticity
140 of the merged eddy became very small, significantly smaller than that of AE2. The circulation and AM of the eddy are
calculated as shown in Fig. 3b. The results are similar to those for the amplitude, i.e., a larger amplitude with larger circulation
and larger AM.



Finally, we calculated the energies of the eddies. Both the EKE and EPE had similar variations before merging.



145 Figure 2. The merging event of surface anticyclonic eddies. The color and contours represent SST and SSHA values, respectively. The eddy boundaries are labelled with dashed curves. The cross and asterisk represent eddy centers identified by fitting method. The dashed lines connecting eddy centers rotates anticyclonically during the merging event.

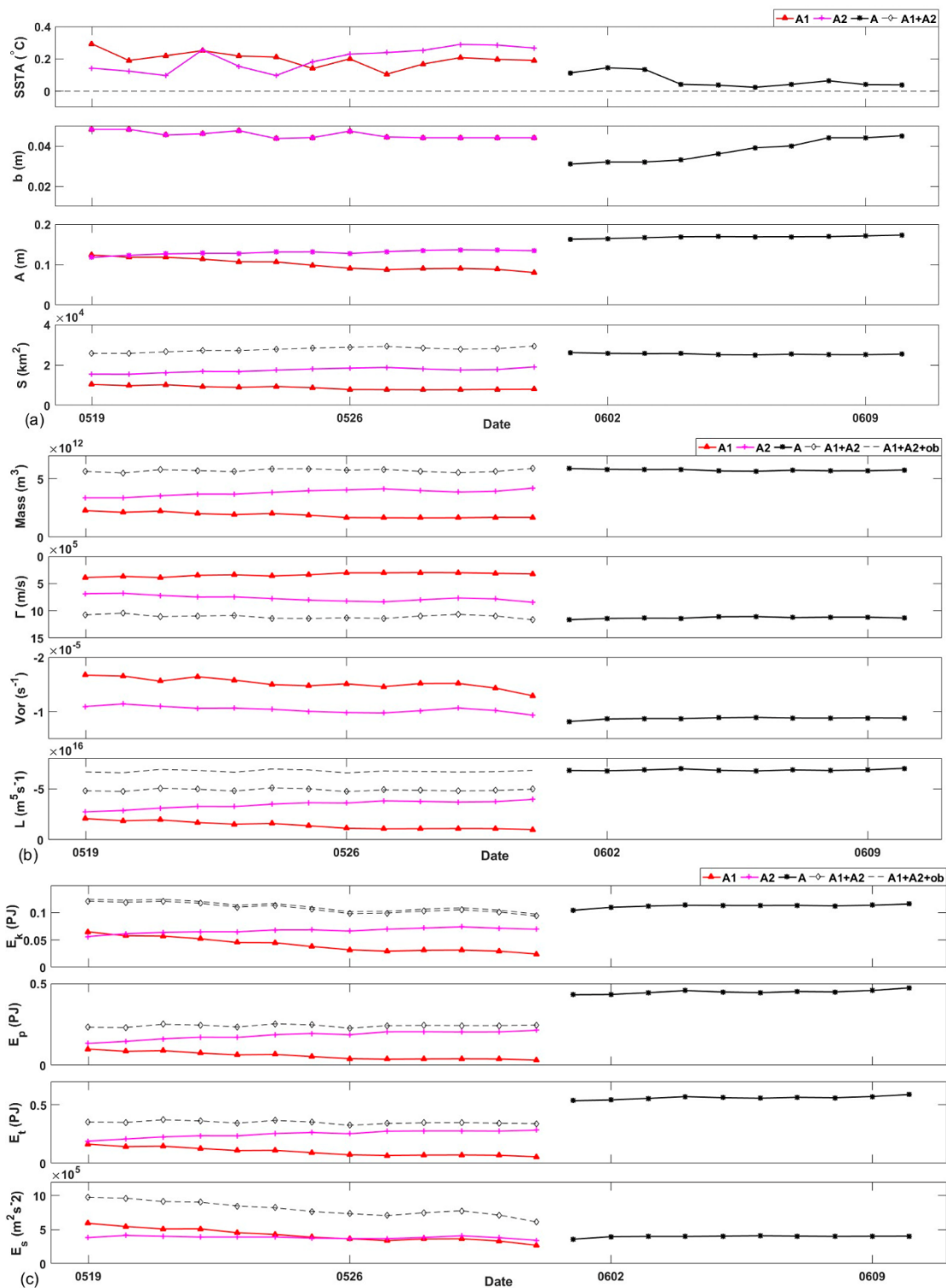




Figure 3. The parameters in the merging event of surface mesoscale eddies. (a) SSTA, background parameter, eddy amplitude, and eddy area, (b) mass, circulation, vorticity, and angular momentum, and (c) EKE, EPE, total mechanical energy, and enstrophy.

155 3.2 Merging of subsurface AEs

The second typical horizontal merging process was between two subsurface anticyclones that occurred in the period from Aug. 29, 2015 to Sept. 22, 2015, in the region between 18° and 23° north latitude, 179° east longitude and 175° west longitude, roughly in the west of the surface vortex merging event of the previous section. In this case, three layers are divided into 0–200 m, 200–400 m, and 400–1000 m, respectively. The mean densities of the layers are 1024.2, 1028.0, and 1030.8 kg/m³, respectively, according to GODAS data for the regions. The height of eddy body H_1 is 200 m, and the upper (lower) surface height h_1 (h_2) is approximately 268 (368) times the eddy amplitude.

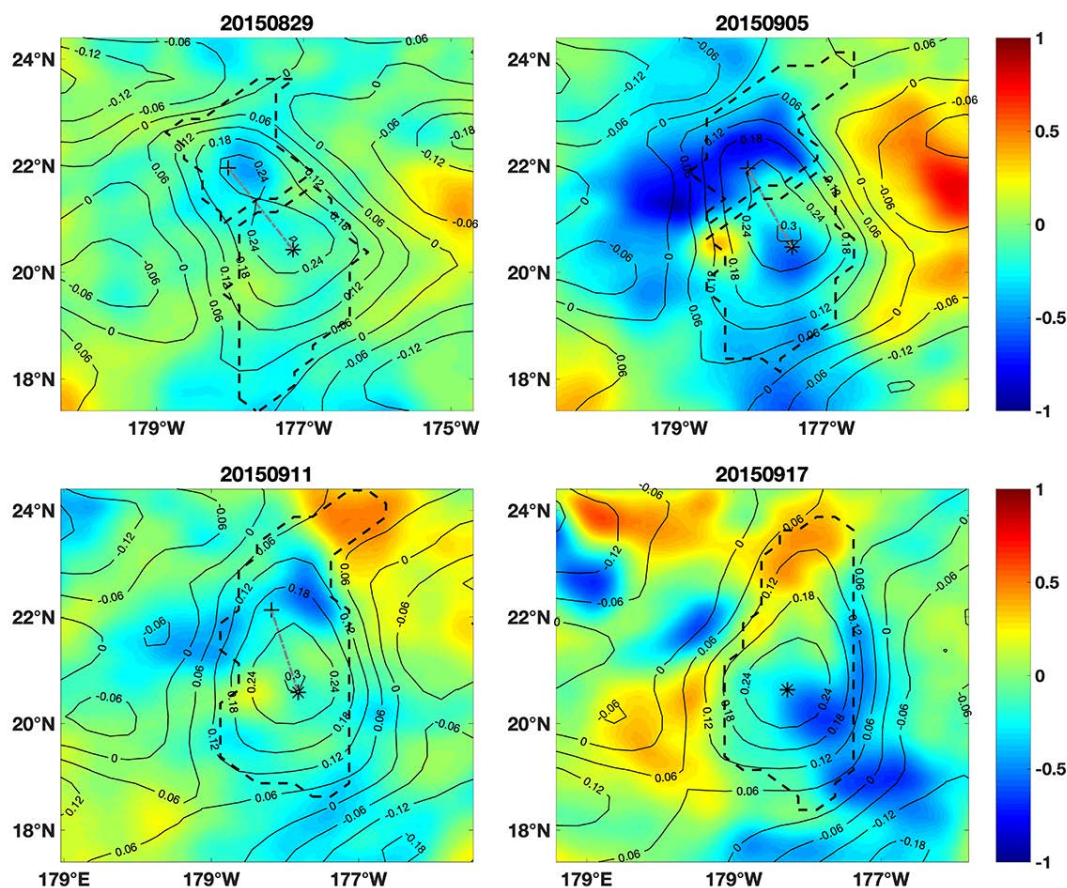


Figure 4. The merging event of subsurface anticyclonic eddies.



At the beginning of the merging, anticyclone A1 was located at approximately 177° north latitude and 20° north latitude, and
165 the other A2 was northwestward alongside A1. Then, A1 and A2 came close to each other along with a clockwise rotation,
and eventually they merged into A on Sept. 13th. Similarly, Fig. 4 shows a series of snapshots of this subsurface-type merging
process. It can be seen that there is a clear cold core, fulfilled by negative SSTA, in each A1, A2, and A at the beginning (top
2 subfigures) and end (bottom 2 subfigures) stages of the process, representing a distinct anticyclonic surface vortex signal.
We also noticed that during the middle of the process, on Sept. 5th, the cold core structures were interrupted by positive SSTA
170 areas, where the small part was between A1 and A2, and the big part with a diameter of approximately 0.5° appeared west of
A1, until two anticyclones merged. On Sept. 14, the cold core structure of merged vortex A was clear again. This may be
caused by the intense mixing effect in eddy–eddy interactions, especially when two like-sign vortices come close to each other.
However, the type of vortex should be determined by the relatively stable continuous stage over a period of time before and
after the merging, so this sudden change would not affect the identification of subsurface AE in this case.

175 To clearly illustrate what occurred for the eddies during the merging process, we first calculated both eddy parameters. It is
obvious that the surface eddy had a positive SSTA, but the subsurface eddy had a negative SSTA. The merged AE had a
positive SSTA (Fig. 5a), i.e., the surface eddy covers the subsurface eddy. The fitted eddy parameters are shown in Fig. 5a.
The first fitted parameter is the vertical shift b representing the background SLA. In this case, b was very small and decreased
by a small amount, from approximately 0.020 m before merging to 0.001 m after merging. The second parameter is the
180 amplitude of the eddy. Before merging, the amplitude of AE1 gradually increased from 0.28 m to 0.30 m, while the amplitude
of AE2 decreased notably from 0.22 m to 0.14 m. After merging, the merged eddy had a amplitude of 0.30 m, similar to that
of AE1. In contrast, the areas of both eddies seldom changed before merging. AE1 had a large area of 2.39×10^4 km², while
AE2 had a smaller area of 1.18×10^4 km².

Next, we calculated the eddy properties using the above parameters. The mass (volume) of the eddies had changes that were
185 similar to those of the eddy area (Fig. 5b). This is because H_1 dominates the whole depth as $h_1 \ll h_2 \ll H_1$. The relative PV
is averaged within each eddy. As shown in Fig. 5b, the vorticity of AE1 varied by a very small amount, and the vorticity of
AE2 gradually decreased before merging. It is noted that the vorticity of AE2 was significantly smaller, although it had a larger
amplitude. This is because vorticity is not only proportional to amplitude, but also inversely proportional to area. After merging,
the vorticity of the merged eddy became very small, significantly smaller than that of AE2. Next, the circulation and AM of
190 the eddy were calculated, as shown in Fig. 5b. The results are similar to those for the amplitude—larger amplitude with larger
circulation and larger AM.

Finally, we calculated the energies of eddies. Both the EKE and EPE had similar variations before merging.

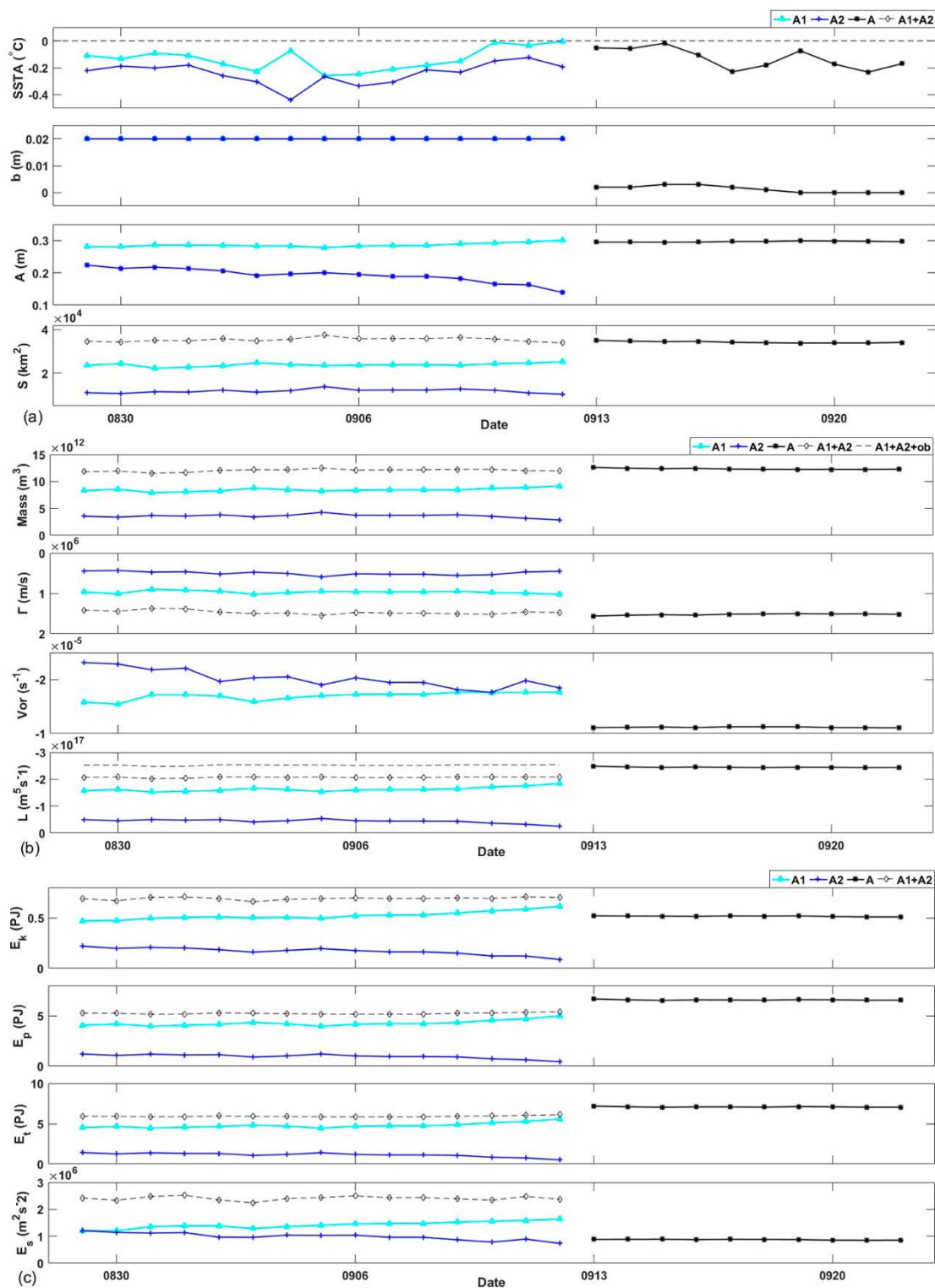




Figure 5. Same parameters as shown in Figure 3, but for subsurface eddies.

195

3.3 Conservation and conversion laws

First, we examine whether the total volume (mass) of eddies was conserved. In the first case, the total volumes pre- and post-merging were $5.71 \pm 0.13 \times 10^{12} \text{ m}^3$ and $5.75 \pm 0.07 \times 10^{12} \text{ m}^3$, respectively. In the second case, the total volumes pre- and post-merging were $1.204 \pm 0.024 \times 10^{13} \text{ m}^3$ and $1.234 \pm 0.013 \times 10^{13} \text{ m}^3$, respectively. As shown in Figs. 3a and 5a, the total volume seldom changes in both cases. It is obvious that the merging events hold the law of conservation of mass.

Next, we find the second conservation law of total circulation. In both cases, the total circulation of the eddies seldom changes. If the circulation is conserved, the flow is referred to as circulation-preserving flow. The circulation-preserving flow has minimum total enstrophy, and minimum dissipation according to the Helmholtz–Rayleigh minimum dissipation theorem. The conservation of total circulation provides a method for calculating the vorticity of the merged eddy, since single eddy PV is not conserved in eddy merging events.

The third conservation law is for total AM. In the first case, the total AM before merging was $4.877 \pm 0.119 \times 10^{16} \text{ m}^5/\text{s}$, while the merged AM was $6.832 \pm 0.082 \times 10^{16} \text{ m}^5/\text{s}$. The merged AM is significantly larger than for pre-merging. Thus, the merged eddy should have some additional sources of AM, which were ignored in previous studies. One possible missing AM source is orbital AM; both eddies co-rotated around the center of mass with an angular speed ω of $-1.9^\circ/\text{day}$, as was mentioned above. This co-rotation provided additional AM of approximately $1.841 \times 10^{16} \text{ m}^5/\text{s}$, or 38% of AM in both eddies. After accounting for the orbital AM to the system, the total AM is approximately $6.718 \times 10^{16} \text{ m}^5/\text{s}$, almost the same as that after merging. Thus, the total AM is conserved by accounting for the orbital AM. In the second case, the total AM before and after merging was $2.070 \pm 0.019 \times 10^{17} \text{ m}^5/\text{s}$ and $2.448 \pm 0.017 \times 10^{17} \text{ m}^5/\text{s}$, respectively. The eddies co-rotated around the center of mass with an angular speed ω of $-1.44^\circ/\text{day}$, which provided an orbital AM of $0.343 \times 10^{17} \text{ m}^5/\text{s}$. In addition, if the water above two subsurface AEs was involved in such orbital AM due to the Taylor–Proudman effect, there should be additional amount of $0.110 \times 10^{17} \text{ m}^5/\text{s}$. According to the Taylor–Proudman theorem, the water was attached to the moving eddies under the geostrophic condition. Thus, the total orbital AM is $0.453 \times 10^{17} \text{ m}^5/\text{s}$, approximately 22% of AM in both eddies. After accounting for the orbital AM to the system, the total AM is approximately $2.523 \times 10^{17} \text{ m}^5/\text{s}$, almost the same as that after merging. In both cases, the orbital AM is nonnegligible.

The law of conservation of total AM was used in previous theoretical models, but without orbital AM. These calculations of total AM assumed that eddies were immersed in quiescent fluid [Pavia and Cushman-Roisin, 1990; Lumpkin et al., 2000], i.e., eddies were motionless before merging. However, this is not true, as two closing eddies would rotate around the center of mass according to fluid dynamics. This rotation was also noted in previous observed eddy merging events [Schultz Tokos et al. 1994; Li et al., 2016]. Because the previous theoretical studies overlooked the orbital AM, the calculations led to an incorrect AM balance between pre- and post-merging.



Although the laws of conservation of total circulation and conservation of total AM are associated with rotation of water, they are somewhat different from the above analysis. The law of conservation of total circulation is only associated with eddy circulation, which is easy to use in applications. However, the conservation of total AM should consider both eddy circulation referring to each eddy center, and the orbital AM referring to the whole system, which is hardly calculated in complex environments.

The total EKE decreased by a small amount after merging in both cases, due to fusion. In the first case, the total EKE decreased from an initial range of 0.121 PJ to 0.094 PJ before merging, then increased from 0.105 PJ to 0.116 PJ after merging. The co-rotation also contributed approximately 0.0034 PJ, a negligible value for total EKE. In the second case, the total EKE decreased from an initial range of 0.692 ± 0.013 PJ to 0.516 ± 0.004 PJ after merging. The co-rotation also contributed a negligible value of 0.0068 PJ in total EKE. Such a decrease in total EKE was noted in a previous study [Nof, 1990], where the EKE is the only component of the energy in theoretical one-layer models.

On the contrary, the total PE increased significantly after merging. In the first case, the total PE increased by approximately 0.207 PJ from an initial range of 0.241 ± 0.008 PJ to 0.448 ± 0.012 PJ. In the second case, the total PE increased by approximately 1.343 PJ from an initial range of 5.229 ± 0.072 PJ to 6.572 ± 0.039 PJ. The large increase of PE cannot be explained by the loss of EKE, since that eddy PE is, in general, an order of magnitude larger than the EKE. Thus, the additional PE from the background environment supplying to the EPE sported the merging events, and the total mechanical energy increased after merging. Both the summer and the fall are favorable for this merging condition in the northern ocean, which consequently leads to less eddies in these seasons, as noted before. This leads to the question of where the huge additional PE came from.

To find the source of the EPE increase, we calculated the change of eddy gravitational PE referring to background sea level with eddy shift parameter b . In the first case (Fig. 3a), b decreased from 0.045 m to 0.038 m after merging. This slightly vertical sink of eddy released approximately 0.401 PJ of gravitational PE, 51.6% of which accounts for the EPE increase. In the second case (Fig. 5a), b decreased from 0.02 m to 0.001 m after merging. The vertical sink of eddies released approximately 2.29 PJ of gravitational PE, 58.6% of which accounts for the EPE increase. Thus, the vertical sink of eddies releasing gravitational PE supported the EPE increase. In addition, it can be deduced that the sink occurred at the level below the eddies; otherwise, it cannot provide enough gravitational PE. For example, if only the surface water sank to the level of b , the released gravitational PE should be much less than the above values. This implies that such gravitational PE may be released from the ocean interior deep below the upper ocean layer. It is also deduced that subsurface eddies might have larger PV than surface eddies. The deeper the eddy is, the larger the gravitational PE it may have. Thus, merged eddies have additional PE conversion from background gravitational PE below the eddies, which has not been noted previously.

Similar to some previous theoretical studies [Gill and Hopfinger 1987; Pavia and Cushman-Roisin, 1990], the total mechanical energy increased after merging in the present work, and vice versa. On the other hand, eddies will merge together if external energy is input into them. A rarely known paper illustrates such a phenomenon [Carnevale and Vallis, 1990].



260 Compared with these studies, our new findings are that the eddy PE dominates the increase of total mechanical energy, and that the EPE increase is converted from the eddy body sink.

265 Though the total circulation was conserved, the mean PV decreased after merging in both cases due to the increase of eddy area. PV conservation was generally assumed in theoretical models [Cushman-Roisin, 1986; Pavia and Cushman-Roisin, 1990; Nof, 1990], although others stressed that the PV of eddies alternated during the interaction of merging [Gill and Hopfinger 1987; Nof and Simon, 1987]. Here we point out that the total circulation conservation other than PV conservation becomes a constraint for eddy merging.

The eddy enstrophy also decreased after merging, even smaller than mean enstrophy of eddies. Because the EKE dissipation rate is proportional to the eddy enstrophy [Li et al., 2018], the merged eddies have a smaller dissipation rate, which might support a potentially longer eddy lifetime.

270 Eddy merging events could play a role in inverse energy cascades from small scale to large scale in two ways. On one hand, it can pump EKE and EPE from small-scale eddies to large-scale eddies. On the other hand, the EKE of large-scale eddies has a lower dissipation rate and longer residence time. Thus, eddy merging behaves like a “large-scale energy pump” in inverse energy cascades.

275 The eddy merging process provides an effective means of mesoscale genesis, which might be a link in the chain for another long-term problem of what physical processes govern the seasonal variability of EKE [Marshall et al., 2002]. In the Northern Hemisphere (e.g., the Gulf Stream region and the Kuroshio Extension region), the ocean is most baroclinically unstable in the mixed layer during late winter [Zhai et al., 2008; Qiu and Chen, 2010], when large-scale atmospheric forcing induce submesoscale eddies via mixed-layer instabilities [Sasaki et al., 2014]. The surface ocean is then strongly stratified due to surface heating and weak vertical mixing in summer [Zhai et al., 2008; Ma et al., 2014]. This strong stratification provides a large PE support for eddy mergers. Eddy merging events can pump the energy from submesoscale eddies into mesoscale eddies and preserves in mesoscale eddies due to weaker dissipation. Consequently, EKE peaks in summer, as observed in previous studies [Zhai et al., 2008; Sasaki et al., 2014]. The strong eddy activity in turn modulates the mixed layer depth [Gaube et al., 2019].

4. Discussion and Conclusion

285 In this paper, the long-term theoretical “energy paradox” of whether the final state of two merging anticyclones contains more energy than the initial state was studied by observation of merging events of ocean mesoscale eddies. Several conservation laws were examined using a two-layer model with parameters fitted from observations, as listed in Table 1. However, only two conservation laws (mass and total circulation) hold with eddy parameters. The third conservation law for AM should also hold if it is accounted for properly by including the orbital AM, a previously overlooked value. Both circulation conservation laws and orbital AM were overlooked in previous theoretical studies. Thus, parts of these previous studies may face some potential challenges in future.

290



In contrast, neither the EKE nor the EPE were conserved after merging. The EKE decreased due to fusion and the EPE increased due to environmental PE conversion related to the vertical shift parameter b . The total mechanical energy increased after merging. According to present results, we can answer the energy paradox that the final merged eddy has more energy than the initial state, mainly contributed from the background gravitational PE below eddies converted to EPE. In addition, eddy merging behaves like a “large-scale energy pump” in inverse energy cascades, which plays an important role in ocean dynamics.

In contrast to previous simple models, there are six eddy parameters—three horizontal (A , L_x , and L_y) and three vertical (H_1 , h_1 , and h_2) in the present model. Two additional eddy parameters referring to the background are also used—vertical shift b and angular speed ω . Additional degrees of freedom were expected to solve the dilemma that parameters are less than conservation laws. All potential conservation laws were expected to simultaneously hold under the condition that degrees of freedom are more than conservation laws. However only limited conservation laws are found in the present results. It is noted that eddy conservation and conversion laws depend on the laws of physical dynamics, even if additional degrees of freedom can be provided in a mathematical model. This implies that the previous theoretical studies could be fully revisited, as physical conservation laws and physical property were not correctly applied in these studies.

305

Table 1. Observed physical quantity changes after merging events and conjectured changes after splitting events

Physical Quantity	Surface Merging	Subsurface Merging	Eddy Splitting
Mass	Conserved	Conserved	Conserved
Circulation	Conserved	Conserved	Conserved
Angular momentum	Conserved	Conserved	Conserved
Potential vorticity	Descended	Descended	Ascended
Enstrophy	Descended	Descended	Ascended
Eddy kinetic energy	Descended	Descended	Ascended
Eddy potential energy	Ascended	Ascended	Descended
Mechanical energy	Ascended	Ascended	Descended

Although only eddy merging events are investigated in this study, it can be hypothesized that similar conservation and conversion laws are also valid in eddy splitting processes. The main difference may be that when a physical quantity ascends in the merging, it descends in the splitting, and vice versa (Table 1).

Finally, the merging and splitting of eddies do not change the total mass, circulation, and AM of the flow field system, but they do change the energy distributions and portions in different scales, which is essential for the energy cascade in multiscale fluid dynamics.



315 *Author contributions.* L.S. designed research; Z.F.W. and L.S. performed research; Q.Y.L. and H.C. contributed data; and L.S. and Z.F.W. wrote the paper.

Competing interests. The authors declare no conflict of interest.

320 *Acknowledgements.* This work is supported by the National Foundation of Natural Science of China (No. 41876013), the National Programme on Global Change and Air-Sea Interaction (GASI-IPOVAI-04). We thank the AVISO for SLA data (<http://www.avisooceanobs.com/>), and APDRC/IPRC for SST data (<http://apdrc.soest.hawaii.edu/data/>), and NOAA for GODAS data (<https://www.esrl.noaa.gov/>). The eddy detection method and the code can be downloaded (<http://www.ocean-sci.net/12/1249/2016/>)

References

- 325 Assassi C, Morel Y, Vandermeirsch F, et al.: An index to distinguish surface-and subsurface-intensified vortices from surface observations. *Journal of Physical Oceanography*, 46, 2529-2552, 2016.
- Bashmachnikov IL, Sokolovskiy MA, Belonenko TV, et al.: On the vertical structure and stability of the Lofoten vortex in the Norwegian Sea. *Deep Sea Research Part I: Oceanographic Research Papers*, 128, 1-27, 2017.
- Behringer DW, Xue Y.: Evaluation of the global ocean data assimilation system at NCEP: The Pacific Ocean[C]/Proc. Eighth
330 Symp. on Integrated Observing and Assimilation Systems for Atmosphere, Oceans, and Land Surface. Seattle, Wash: AMS 84th Annual Meeting, Washington State Convention and Trade Center, 2004.
- Carnevale GF, Vallis GK. Pseudo-advective relaxation to stable states of inviscid two-dimensional fluids. *Journal of Fluid Mechanics*, 213, 549-571, 1990.
- Chelton DB, Schlax MG, Samelson RM.: Global observations of nonlinear mesoscale eddies. *Progress in oceanography*, 91,
335 167-216, 2011.
- Cushman-Roisin B.: On the role of filamentation in the merging of anticyclonic lenses. *Journal of physical oceanography*, 19, 253-258, 1989.
- Cresswell GR.: The coalescence of two East Australian Current warm-core eddies. *Science*, 215, 161-164, 1982.
- Dong C, McWilliams JC, Liu Y, et al.: Global heat and salt transports by eddy movement. *Nature communications*, 5, 3294,
340 2014.
- Donlon CJ, Martin M, Stark J, et al.: The operational sea surface temperature and sea ice analysis (OSTIA) system. *Remote Sensing of Environment*, 116, 140-158, 2012.
- Ducet N, Le Traon PY, Reverdin G.: Global high-resolution mapping of ocean circulation from TOPEX/Poseidon and ERS-1 and-2. *Journal of Geophysical Research: Oceans*, 105, 19477-19498, 2000.
- 345 Griffiths RW, Hopfinger EJ. : Coalescing of geostrophic vortices. *Journal of Fluid Mechanics*, 178, 73-97, 1987.



- Gaube, P., McGillicuddy Jr., D. J., & Moulin, A. J. : Mesoscale eddies modulate mixed layer depth globally. *Geophysical Research Letters*, 46, 1505-1512. <https://doi.org/10.1029/2018GL080006>, 2019.
- Li C, Zhang Z, Zhao W, et al.: A statistical study on the subthermocline submesoscale eddies in the northwestern Pacific Ocean based on Argo data. *Journal of Geophysical Research: Oceans*, 122, 3586-3598, 2017.
- 350 Li Q, Sun L. : Watershed strategy for oceanic mesoscale eddy splitting. *Ocean Science*, 11, 269-273, 2015.
- Li Q, Sun L, Liu S, et al. : A new mononuclear eddy identification method with simple splitting strategies. *Remote sensing letters*, 5, 65-72, 2014.
- Li Q, Sun L, Lin S.: GEM: a dynamic tracking model for mesoscale eddies in the ocean. *Ocean Science*, 12, 1249-1267, 2016.
- Li Q, Sun L, Xu C. : The Lateral Eddy Viscosity Derived from the Decay of Oceanic Mesoscale Eddies. *Open Journal of Marine Science*, 8, 152-172, 2018.
- 355 Lumpkin R, Flament P, Kloosterziel R, et al.: Vortex Merging in a 1½-Layer Fluid on an f Plane. *Journal of physical oceanography*, 30, 233-242, 2000.
- Ma X, Jing Z, Chang P, et al.: Western boundary currents regulated by interaction between ocean eddies and the atmosphere. *Nature*, 535(7613), 533-537, 2016.
- 360 McGillicuddy DJ.: Eddies masquerade as planetary waves. *Science*, 334, 318-319, 2011.
- Nof D, Simon LM.: Laboratory experiments on the merging of nonlinear anticyclonic eddies. *Journal of physical oceanography*, 17, 343-357, 1987.
- Nof D. : The role of angular momentum in the splitting of isolated eddies. *Tellus A: Dynamic Meteorology and Oceanography* 42, 469-481, 1990.
- 365 Nof D. : The fusion of isolated nonlinear eddies. *Journal of physical oceanography*, 18, 887-905, 1988.
- Pavia EG, Cushman-Roisin B.: Merging of frontal eddies. *Journal of physical oceanography*, 20, 1886-1906, 1990.
- Pujol MI, Faugère Y, Taburet G, et al. : DUACS DT2014: the new multi-mission altimeter data set reprocessed over 20 years. *Ocean Science*, 12, 1067-1090, 2016.
- Qiu B, Chen S.: Eddy-mean flow interaction in the decadal modulating Kuroshio Extension system. *Deep Sea Research Part*
- 370 *II: Topical Studies in Oceanography*, 57, 1098-1110, 2010.
- Sangrà P, Pelegrí JL, Hernández-Guerra A, et al. : Life history of an anticyclonic eddy. *Journal of Geophysical Research: Oceans*, 110, 2156-2202, 2005.
- Sasaki H, Klein P, Sasai Y, et al. : Regionality and seasonality of submesoscale and mesoscale turbulence in the North Pacific Ocean. *Ocean Dynamics*, 67, 1195-1216, 2017.
- 375 Schultz Tokos KL, Hinrichsen HH, Zenk W. : Merging and migration of two meddies. *Journal of Physical Oceanography* 24, 2129-2141, 1994.
- Wang Z, Li Q, Sun L, et al. : The most typical shape of oceanic mesoscale eddies from global satellite sea level observations. *Frontiers of Earth Science*, 9, 202-208, 2015.



- Yi J, Du Y, Zhou C, et al. : Automatic identification of oceanic multieddy structures from satellite altimeter datasets. IEEE
380 Journal of Selected Topics in Applied Earth Observations and Remote Sensing, 8,1555-1563, 2015.
- Zhang Z, Li P, Xu L, et al. : Subthermocline eddies observed by rapid-sampling Argo floats in the subtropical northwestern
Pacific Ocean in Spring 2014. Geophysical Research Letters, 42, 6438-6445, 2015.
- Marshall J, Jones H, Karsten R, et al. : Can eddies set ocean stratification? Journal of physical oceanography, 32, 26-38, 2002.
- Zhai X, Greatbatch RJ, Kohlmann JD. On the seasonal variability of eddy kinetic energy in the Gulf Stream region.
385 Geophysical Research Letters, 35(24), 745-750, 2008.
- Zhang Z, Wang W, Qiu B. : Oceanic mass transport by mesoscale eddies. Science, 345, 322-324, 2014.